



Structural and dielectric properties of $\text{Bi}_2\text{Zn}_{2/3}\text{Nb}_{4/3}\text{O}_7$ thin films prepared by pulsed laser deposition at low temperature for embedded capacitor applications

Xiaohua Zhang, Wei Ren*, Peng Shi, M. Saeed Khan, Xiaofeng Chen, Xiaoqing Wu, Xi Yao

Electronic Materials Research Laboratory, Key Laboratory of the Ministry of Education & International Center for Dielectric Research, Xi'an Jiaotong University, Xi'an 710049, China

ARTICLE INFO

Article history:

Received 8 March 2011

Received in revised form 28 June 2011

Accepted 30 June 2011

Available online 7 July 2011

Keywords:

$\text{Bi}_2\text{Zn}_{2/3}\text{Nb}_{4/3}\text{O}_7$ thin films

Low temperature

Pulsed laser deposition

Dielectric properties

ABSTRACT

$\text{Bi}_2\text{Zn}_{2/3}\text{Nb}_{4/3}\text{O}_7$ thin films were deposited on Pt/TiO₂/SiO₂/Si(100) substrates at a room temperature under the oxygen pressure of 1–10 Pa by pulsed laser deposition. $\text{Bi}_2\text{Zn}_{2/3}\text{Nb}_{4/3}\text{O}_7$ thin films were then post-annealed below 200 °C in a rapid thermal process furnace in air for 20 min. The dielectric and leakage current properties of $\text{Bi}_2\text{Zn}_{2/3}\text{Nb}_{4/3}\text{O}_7$ thin films are strongly influenced by the oxygen pressure during deposition and the post-annealing temperature. $\text{Bi}_2\text{Zn}_{2/3}\text{Nb}_{4/3}\text{O}_7$ thin films deposited under 1 Pa oxygen pressure and then post-annealed at a temperature of 150 °C show uniform surface morphologies. Dielectric constant and loss tangent are 57 and 0.005 at 10 kHz, respectively. The high resolution TEM image and the electron diffraction pattern show that nano crystallites exist in the amorphous thin film, which may be the origin of high dielectric constant in the $\text{Bi}_2\text{Zn}_{2/3}\text{Nb}_{4/3}\text{O}_7$ thin films deposited at low temperatures. Moreover, $\text{Bi}_2\text{Zn}_{2/3}\text{Nb}_{4/3}\text{O}_7$ thin film exhibits the excellent leakage current characteristics with a high breakdown strength and the leakage current density is approximately 1×10^{-7} A/cm² at an applied bias field of 300 kV/cm. $\text{Bi}_2\text{Zn}_{2/3}\text{Nb}_{4/3}\text{O}_7$ thin films are potential materials for embedded capacitor applications.

© 2011 Elsevier B.V. All rights reserved.

1. Introduction

In microelectronics industry, device miniaturization, low-power operation and high reliability are new challenges [1]. Embedding thin-film capacitors with high permittivity dielectrics into printed circuit boards (PCBs) is one of the methods to approach these goals [2–4]. In integrated circuit packages, the polymer substrates cannot sustain the temperature of more than 200 °C, which limits the thermal process of capacitor materials [2]. Ferroelectric thin films have been investigated for such applications [2,3,5,6]. But ferroelectric materials with high dielectric constants can only be obtained for the crystallite phase, which usually requires a high temperature (>550 °C). However, ferroelectric thin films deposited at or near room temperature exhibit very low dielectric constants and high dielectric losses [5,6]. Moreover, the conventional paraelectric oxides such as SiO₂ (~3.9), Ta₂O₅ (~25) and Al₂O₃ (~9) can be fabricated at low temperature but they have very low dielectric constants [1–3]. $\text{Bi}_2\text{Zn}_{2/3}\text{Nb}_{4/3}\text{O}_7$ is one of the candidate materials, which is feasible for PCB applications. $\text{Bi}_2\text{Zn}_{2/3}\text{Nb}_{4/3}\text{O}_7$ possesses a monoclinic zirconolite structure, being different from its counterpart, cubic pyrochlore $\text{Bi}_{1.5}\text{Zn}_{1.0}\text{Nb}_{1.5}\text{O}_7$ [7–9]. Moreover, monoclinic $\text{Bi}_2\text{Zn}_{2/3}\text{Nb}_{4/3}\text{O}_7$ exhibits much higher quality

factor ($Q \sim 1000$) than that of cubic $\text{Bi}_{1.5}\text{Zn}_{1.0}\text{Nb}_{1.5}\text{O}_7$ ($Q \sim 35$) at a microwave range [10]. Ren et al. reported the crystallized $\text{Bi}_2\text{Zn}_{2/3}\text{Nb}_{4/3}\text{O}_7$ thin films synthesized by a metal-organic deposition (MOD) process with a dielectric constant of 80 and loss tangent of 0.004 at 10 kHz, respectively [11].

In this paper, $\text{Bi}_2\text{Zn}_{2/3}\text{Nb}_{4/3}\text{O}_7$ thin films were deposited on Pt/TiO₂/SiO₂/Si(100) substrates by pulsed laser deposition (PLD) process at a room temperature, and then post-annealed at a temperature below 200 °C. The influences of annealing temperature and oxygen pressure on microstructure, dielectric properties and leakage current characteristics of $\text{Bi}_2\text{Zn}_{2/3}\text{Nb}_{4/3}\text{O}_7$ thin films have been investigated.

2. Experimental procedure

The monoclinic $\text{Bi}_2\text{Zn}_{2/3}\text{Nb}_{4/3}\text{O}_7$ ceramic targets were prepared using a conventional solid-state reaction method and then sintered at 960 °C for 4 h. $\text{Bi}_2\text{Zn}_{2/3}\text{Nb}_{4/3}\text{O}_7$ thin films were deposited on Pt/TiO₂/SiO₂/Si(100) substrate by a PLD process. A KrF excimer laser (COMPex Pro 205, Coherent Lambda Physik) at a wavelength of 248 nm with pulse width of 30 ns and repetition rate of 3 Hz was used. The laser energy was set at 200 mJ/pulse. The deposition was carried out for 40 min at room temperature and the oxygen pressure was set in a range of 1–10 Pa. Then, $\text{Bi}_2\text{Zn}_{2/3}\text{Nb}_{4/3}\text{O}_7$ thin films were post-annealed from 100 °C to 200 °C in a rapid thermal process furnace in air for 20 min.

The crystallinity of the $\text{Bi}_2\text{Zn}_{2/3}\text{Nb}_{4/3}\text{O}_7$ thin film was characterized by using an X-ray diffractometer with Cu K α radiation (XRD, D/Max-2400, Rigaku) and a high resolution transmission electron microscope (TEM, JEM-3010, JEOL). The surface morphological features were studied by an atomic force microscope (AFM, Nanoscope, Veeco) and a scanning electron microscope (SEM, JSM-7000F, JEOL). Thickness of the films was measured by a stylus surface profiler (Dektak 6M, Veeco).

* Corresponding author. Tel.: +86 29 82666873; fax: +86 29 82668794.
E-mail address: wren@mail.xjtu.edu.cn (W. Ren).

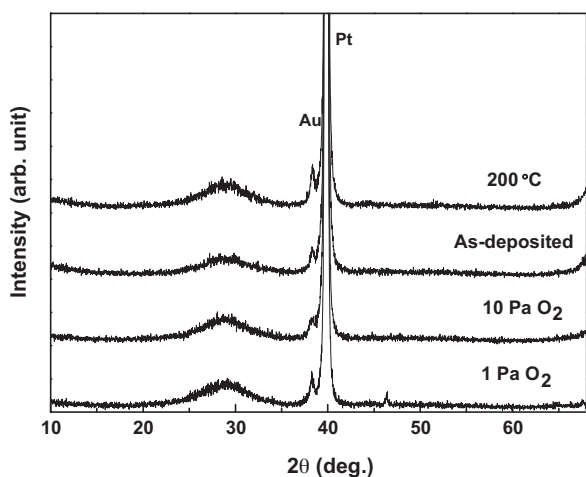


Fig. 1. X-ray diffraction patterns of $\text{Bi}_2\text{Zn}_{2/3}\text{Nb}_{4/3}\text{O}_7$ thin films as functions of annealing temperature and oxygen pressure.

For measuring electrical properties, Au top electrodes with a diameter of 0.5 mm were deposited using DC sputtering via a shadow mask to form a metal-insulator-metal (MIM) structure. The dielectric properties were investigated by using a precision impedance analyzer (4294A, Agilent). Current–voltage (I – V) characteristics were examined with a semiconductor characterization system (4200-SCS, Keithley).

3. Results and discussion

Fig. 1 shows XRD patterns of $\text{Bi}_2\text{Zn}_{2/3}\text{Nb}_{4/3}\text{O}_7$ thin films deposited under different oxygen pressures and annealed at different temperatures. All thin films show weaker and broader peaks, which are near 29° in XRD patterns and the d -values

of the broad diffraction peak are about 3.09. It was found that the broad diffraction peak in the XRD patterns corresponds to the strongest (221) peak of the monoclinic zirconolite structure $\text{Bi}_2\text{Zn}_{2/3}\text{Nb}_{4/3}\text{O}_7$. The high energy particle collisions during deposition in PLD process probably produce the small grains (typically in a nanometer scale) and highly disordered amorphous phase in the films, which have also been identified by the analysis of TEM in the Bi-based pyrochlore films fabricated at low temperature [3]. In general, amorphous paraelectric (such as Ta_2O_5 , Al_2O_3 and SiO_2) thin films fabricated at low temperature usually exhibit low dielectric constants (<25) [2]. However, in the Bi-based thin films, such as $\text{Bi}_{1.5}\text{Zn}_{1.0}\text{Nb}_{1.5}\text{O}_7$, $\text{Bi}_2\text{Zn}_{2/3}\text{Nb}_{4/3}\text{O}_7$, $\text{Bi}_2\text{Mg}_{2/3}\text{Nb}_{4/3}\text{O}_7$, if some nanosized crystallites are present in thin films, these films exhibit high dielectric constants [2–4,12].

Surface morphologies of $\text{Bi}_2\text{Zn}_{2/3}\text{Nb}_{4/3}\text{O}_7$ thin films post-annealed at different temperatures do not show any distinct differences, but they are remarkably influenced by the oxygen pressure during deposition. **Fig. 2** shows SEM surface morphologies of $\text{Bi}_2\text{Zn}_{2/3}\text{Nb}_{4/3}\text{O}_7$ thin films deposited under various oxygen pressures and annealed at 150°C . It can be seen in **Fig. 2(a)** and **2(b)** that the thin films deposited at low oxygen pressures of 1 Pa and 4 Pa show dense, crack-free and homogenous surfaces. With increasing oxygen pressure to 7 Pa, the surface morphology of the thin film shows a distinct change. The thin film exhibits a rough surface with large clusters of particles and a lot of micro-cracks between particles, as shown in **Fig. 2(c)**. With further increase of oxygen pressure to 10 Pa, much larger clusters of particles can be observed and micro-cracks become more evident. The surface roughness and deposition rate of $\text{Bi}_2\text{Zn}_{2/3}\text{Nb}_{4/3}\text{O}_7$ films show little variation with post-annealing temperature, but they increase significantly with increasing oxygen pressure, as shown in **Fig. 3**.

Surface morphology and roughness, as well as deposition rate are correlative to the energy of the ablated species. The PLD process

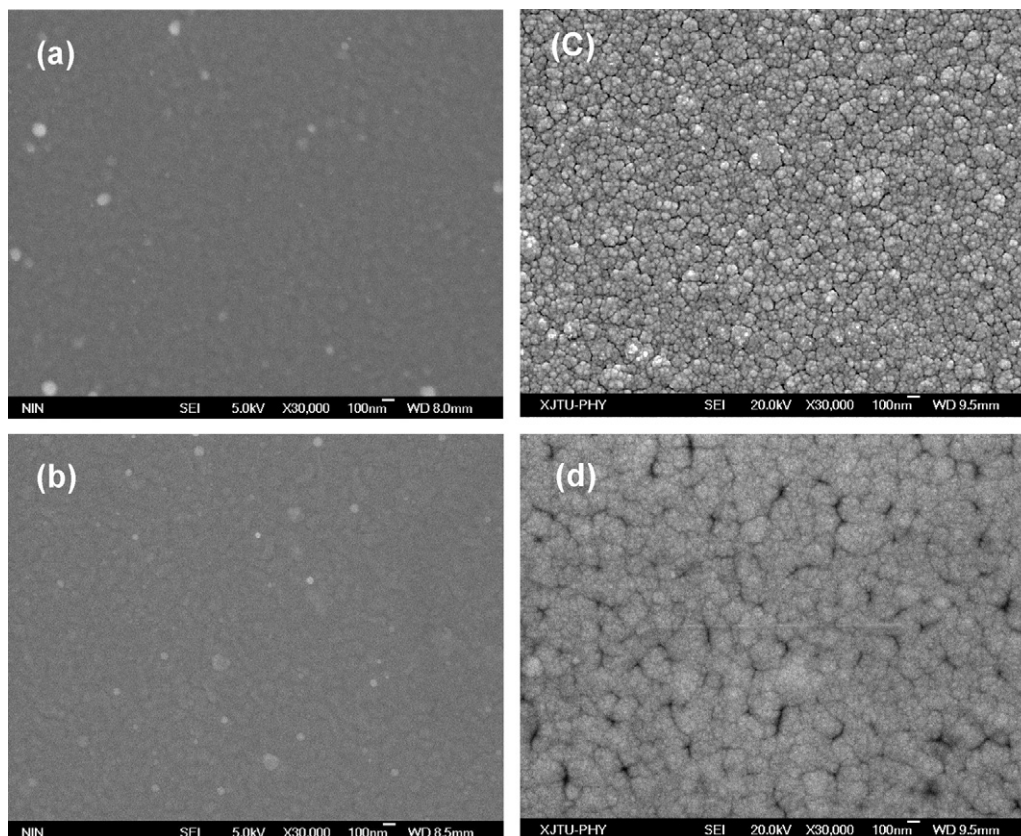


Fig. 2. Surface morphologies of $\text{Bi}_2\text{Zn}_{2/3}\text{Nb}_{4/3}\text{O}_7$ thin films deposited under oxygen pressures of (a) 1 Pa, (b) 4 Pa, (c) 7 Pa and (d) 10 Pa.

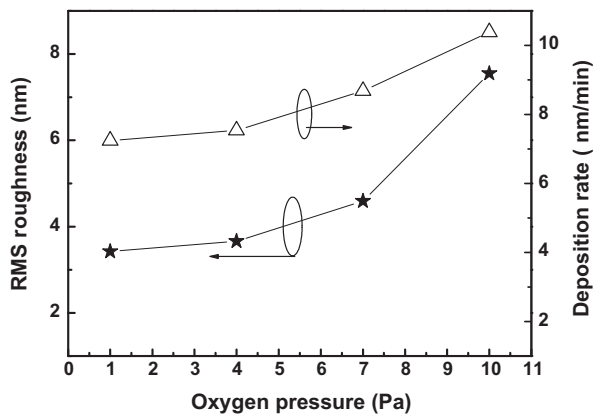


Fig. 3. Surface roughness and deposition rate of $\text{Bi}_2\text{Zn}_{2/3}\text{Nb}_{4/3}\text{O}_7$ thin films deposited under different oxygen pressures.

usually involves following three stages: plasma plume generation, transportation and condensation [13]. In the second stage, the ablated species lose their energy through random collisions with atoms/molecules of the background oxygen. As the oxygen pressure in the deposition chamber varies in the range of 1–10 Pa, both the collision probability and energy loss change accordingly. At low oxygen pressure of 1–4 Pa, most of the kinetic energy and internal energy of the ablated species are kept due to less collision. These energies transform into migration energy on the substrate, which results in the formation of dense thin films because the atoms have enough energy for self-arrangement on the substrate. However, with the increase of oxygen pressure, both kinetic energy and internal energy of the ablated species significantly decrease as a result of frequent collisions [2]. The ablated species cannot arrive in the ideal locations, and hence form the large clusters and micro-cracks in the thin films. The deposition rate of the thin films increases with increasing oxygen pressure. Under low oxygen pressure, the ablated species have high energy and a part of the incident particles with high energy tends to desorption from the substrate due to the effect of re-sputtering, which leads to a low deposition rate. With an increase of oxygen pressure, the ablated species lose partial energy before reaching to the substrate due to frequent collisions. Hence, the number of adatoms on the substrate increases, which results in the increase of the deposition rate [14]. For the same deposition time of 40 min, the film thickness is varied from 200 to 400 nm, which is attributed to the variation of oxygen pressure.

The dielectric properties of $\text{Bi}_2\text{Zn}_{2/3}\text{Nb}_{4/3}\text{O}_7$ thin films deposited under an oxygen pressure of 4 Pa and annealed at different temperatures are shown in Fig. 4. The as-deposited $\text{Bi}_2\text{Zn}_{2/3}\text{Nb}_{4/3}\text{O}_7$ thin film shows dielectric constant of 53.6 and loss tangent of 0.01 at 10 kHz, respectively. The dielectric constant of $\text{Bi}_2\text{Zn}_{2/3}\text{Nb}_{4/3}\text{O}_7$ thin films gradually increases with post-annealing temperature and reaches a maximum at 150 °C, and then decreases at higher temperature up to 200 °C. The decrease in the dielectric constant for the film annealed at 200 °C can be attributed to the high temperature migration of Bi [2]. The migration reduces the Bi–O contribution to the overall polarization in the $\text{Bi}_2\text{Zn}_{2/3}\text{Nb}_{4/3}\text{O}_7$ thin film, which results in the drop of dielectric constant [2]. The dielectric constant and loss tangent of the film annealed at 150 °C are 60 and 0.007 at 10 kHz, respectively.

Fig. 5 shows the dielectric properties of $\text{Bi}_2\text{Zn}_{2/3}\text{Nb}_{4/3}\text{O}_7$ thin films deposited under various oxygen pressures and annealed at 150 °C. The dielectric properties of $\text{Bi}_2\text{Zn}_{2/3}\text{Nb}_{4/3}\text{O}_7$ thin films show a strong dependence on oxygen pressure. The thin films deposited under low oxygen pressure exhibit superior dielectric properties. However, the dielectric constant decreases and dielectric loss tangent increases at higher oxygen pressure. The $\text{Bi}_2\text{Zn}_{2/3}\text{Nb}_{4/3}\text{O}_7$ thin

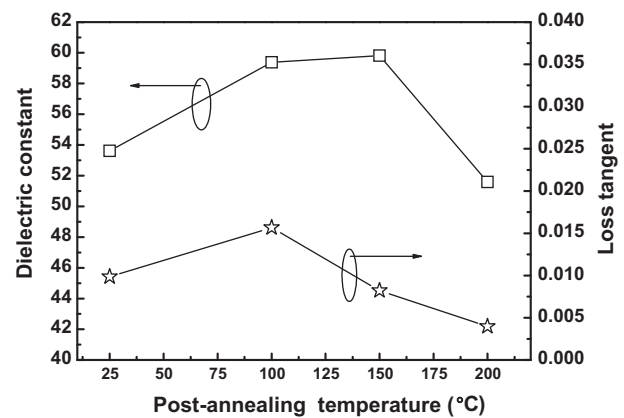


Fig. 4. Dielectric constant and loss tangent of $\text{Bi}_2\text{Zn}_{2/3}\text{Nb}_{4/3}\text{O}_7$ thin films as a function of post-annealing temperature at a measured frequency of 10 kHz.

films deposited under 1 Pa and 4 Pa exhibit high dielectric constants of 57 and 60, and very low loss tangent of 0.005 and 0.007 at 10 kHz, respectively. While the $\text{Bi}_2\text{Zn}_{2/3}\text{Nb}_{4/3}\text{O}_7$ thin films deposited under 10 Pa show lower dielectric constant of 28 and high loss tangent of 0.08 at 10 kHz, which attributes to the presence of large clusters of particles and micro-cracks. It can be concluded that the dense film is helpful to improve the dielectric properties of the films.

The high resolution transmission electron microscope (TEM) was used to analyze the microstructure of the $\text{Bi}_2\text{Zn}_{2/3}\text{Nb}_{4/3}\text{O}_7$ thin film. Fig. 6(a) and (b) shows the TEM plane-view image and the electron diffraction pattern of the $\text{Bi}_2\text{Zn}_{2/3}\text{Nb}_{4/3}\text{O}_7$ thin film deposited under 1 Pa oxygen pressure and then post-annealed at 150 °C. As shown in Fig. 6(a), an incipient crystallization (black particles) is clearly observed. The broad diffraction rings of the film in Fig. 6(b) also indicate that there are nanosized crystallites in the thin film. The area with the black particles is further enlarged and is shown in the inset of Fig. 6(a). The crystallinity within the $\text{Bi}_2\text{Zn}_{2/3}\text{Nb}_{4/3}\text{O}_7$ thin film is clearly identified and the crystallite particle size is approximately 4 nm. The result is also consistent to the analysis of the XRD patterns. The high dielectric constant of $\text{Bi}_2\text{Zn}_{2/3}\text{Nb}_{4/3}\text{O}_7$ thin films may be attributed to the nanosized crystallites in the thin films.

Fig. 7 shows I – V characteristics of $\text{Bi}_2\text{Zn}_{2/3}\text{Nb}_{4/3}\text{O}_7$ thin films as a function of post-annealing temperature. It can be seen that the leakage characteristics are remarkably improved with post-annealing. The thin films show an abrupt increase of leakage current densities with increasing applied field, except the thin film being annealed at 150 °C. In particular, the thin film annealed at 150 °C exhibits

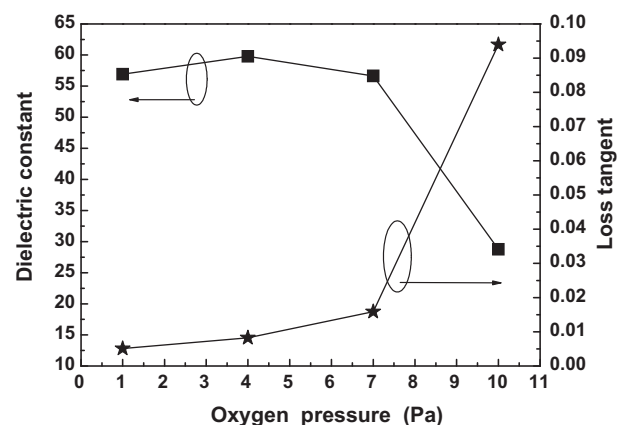


Fig. 5. Dielectric constant and loss tangent of $\text{Bi}_2\text{Zn}_{2/3}\text{Nb}_{4/3}\text{O}_7$ thin films as a function of oxygen pressure during deposition and measured at a frequency of 10 kHz.

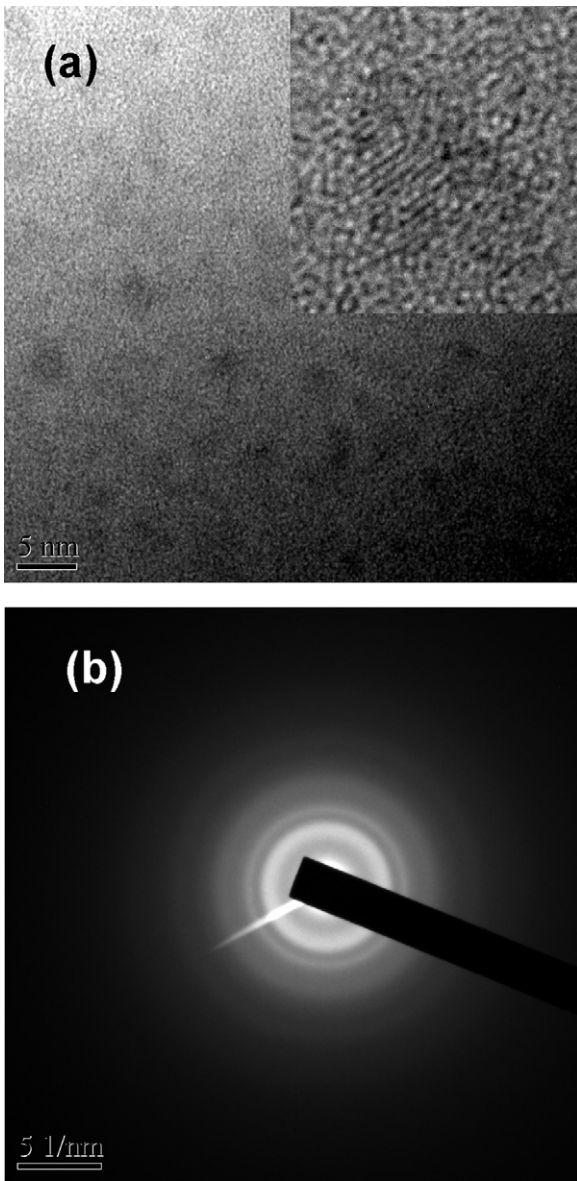


Fig. 6. (a) Plane-view TEM image and (b) electron diffraction pattern of $\text{Bi}_2\text{Zn}_{2/3}\text{Nb}_{4/3}\text{O}_7$ thin film deposited at 1 Pa oxygen pressure and annealed at 150 °C. The inset in Fig. 6(a) shows an enlargement of TEM image (The black particle area in the plane-view TEM image).

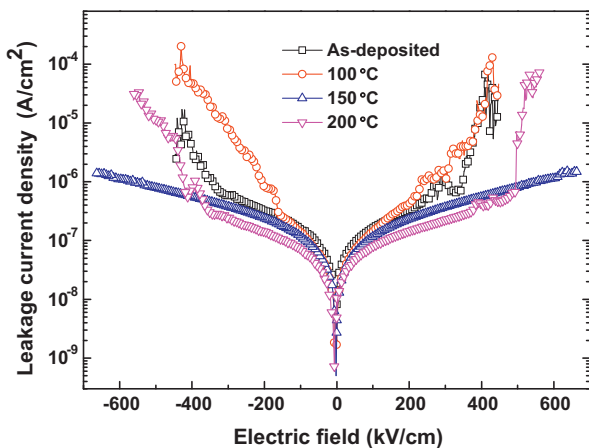


Fig. 7. Leakage current density versus applied bias field for $\text{Bi}_2\text{Zn}_{2/3}\text{Nb}_{4/3}\text{O}_7$ thin films annealed at different temperatures.

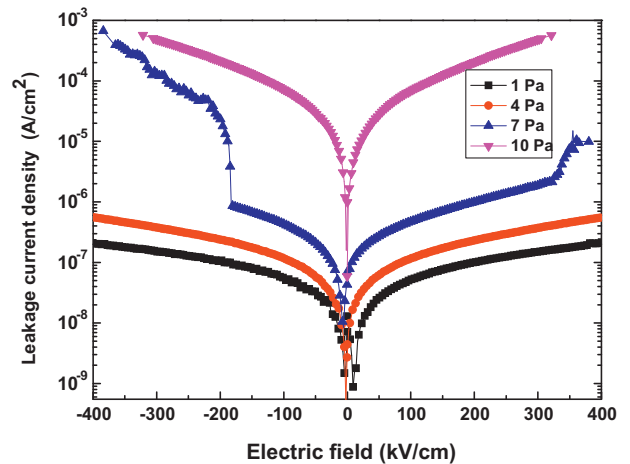


Fig. 8. Leakage current density versus applied bias field for $\text{Bi}_2\text{Zn}_{2/3}\text{Nb}_{4/3}\text{O}_7$ thin films deposited at various oxygen pressures.

an improved leakage current characteristic and the leakage current density of less than $4 \times 10^{-7} \text{ A/cm}^2$ at 300 kV/cm and a high breakdown field of 700 kV/cm. Fig. 8 shows I - V characteristics of $\text{Bi}_2\text{Zn}_{2/3}\text{Nb}_{4/3}\text{O}_7$ thin films deposited at various oxygen pressures. The leakage characteristics show a strong dependence on oxygen pressure. The leakage current density increases remarkably with oxygen pressure. The low leakage current is one of basic requirement for a good dielectric thin film. The thin film deposited at the low oxygen pressure of 1 Pa exhibits very low leakage current which is approximately $1 \times 10^{-7} \text{ A/cm}^2$ at an applied bias field of 300 kV/cm. These results suggest that $\text{Bi}_2\text{Zn}_{2/3}\text{Nb}_{4/3}\text{O}_7$ thin films are a potential candidate for embedded passive components in the PCB applications.

4. Conclusions

$\text{Bi}_2\text{Zn}_{2/3}\text{Nb}_{4/3}\text{O}_7$ thin films prepared at low temperature by PLD exhibit large dielectric constant, low loss tangent and low leakage current characteristics, which make them a promising candidate material for embedded capacitors. The structures and properties of $\text{Bi}_2\text{Zn}_{2/3}\text{Nb}_{4/3}\text{O}_7$ thin films are strongly influenced by post-annealing temperature and oxygen pressure. The dielectric constant and the loss tangent of the thin films deposited under an oxygen pressure of 1 Pa and post-annealed at 150 °C are 57 and 0.005 at 10 kHz, respectively. The high dielectric constant of $\text{Bi}_2\text{Zn}_{2/3}\text{Nb}_{4/3}\text{O}_7$ thin films deposited at low temperature may be attributed to the nano-size crystallites in the films. The leakage current density is approximately $1 \times 10^{-7} \text{ A/cm}^2$ at an applied field of 300 kV/cm.

Acknowledgements

This work is supported by the Natural Science Foundation of China (grant no. 90923001), the International Science & Technology Cooperation Program of China (grant no. 2010DFB13640) and the Shaanxi Province International Collaboration Program (grant nos. 2009KW-12 and 2010KW-09).

References

- [1] A.M. Stoneham, *J. Non-Cryst. Solids* 303 (2002) 114–122.
- [2] J.H. Park, W.S. Lee, N.J. Seong, S.G. Yoon, S.H. Son, H.M. Chung, J.S. Moon, H.J. Jin, S.E. Lee, J.W. Lee, H.D. Kang, Y.K. Chung, Y.S. Oh, *Appl. Phys. Lett.* 88 (2006) 192902.
- [3] J.H. Park, C.J. Xian, N.J. Seong, S.G. Yoon, S.H. Son, H.M. Chung, J.S. Moon, H.J. Jin, S.E. Lee, J.W. Lee, H.D. Kang, Y.K. Chung, Y.S. Oh, *Appl. Phys. Lett.* 89 (2006) 232910.

- [4] J.K. Ahn, H.W. Kim, K.C. Ahn, S.G. Yoon, S.H. Son, H.M. Jung, J.S. Moon, H.J. Jin, S.E. Lee, J.W. Lee, Y.K. Chung, Y.S. Oh, *Integrated Ferroelectrics* 95 (2007) 187–195.
- [5] J.P. Maria, K. Cheek, S. Streiffer, S.H. Kim, G. Dunn, A. Kingon, *J. Am. Ceram. Soc.* 84 (2001) 2436–2438.
- [6] F. El Kamel, P. Gonon, F. Jomni, *Thin Solid Films* 504 (2006) 201–204.
- [7] I. Levina, T.G. Amos, J.C. Nino, T.A. Vanderah, I.M. Reaney, C.A. Randall, T.L. Michael, *J. Mater. Res.* 17 (2002) 1406–1411.
- [8] X.H. Zhang, W. Ren, P. Shi, X.F. Chen, X.Q. Wu, *Appl. Surf. Sci.* 256 (2010) 1861–1865.
- [9] X.H. Zhang, W. Ren, P. Shi, X.F. Chen, X.Q. Wu, *Appl. Surf. Sci.* 256 (2010) 6607–6611.
- [10] H. Wang, S. Kamba, M.L. Zhang, X. Yao, S. Denisov, F. Kadlec, J. Petzelt, *J. Appl. Phys.* 100 (2006) 034109.
- [11] W. Ren, S. Trolier-McKinsky, C.A. Randall, T.S. Shrout, *J. Appl. Phys.* 89 (2001) 767–774.
- [12] J. Ryu, K.Y. Kim, J.J. Choi, B.D. Hahn, W.H. Yoon, D.S. Park, Chan Park, *J. Am. Ceram. Soc.* 91 (2008) 3399–3401.
- [13] C.R. Cho, A. Grishin, *J. Appl. Phys.* 87 (2000) 4439–4448.
- [14] M. Tyunina, J. Levoska, S. Leppavuori, *J. Appl. Phys.* 83 (1998) 5489–5496.